THE JOURNAL OF BIOLOGICAL CHEMISTRY VOL. 282, NO. 13, pp. 9581–9590, March 30, 2007

Oxaloacetate Hydrolase, the C–C Bond Lyase of Oxalate Secreting Fungi*

Received for publication, September 20, 2006, and in revised form, January 22, 2007 Published, JBC Papers in Press, January 23, 2007, DOI 10.1074/jbc.M608961200

Ying Han[‡1], Henk-Jan Joosten[§1], Weiling Niu[‡], Zhiming Zhao[‡], Patrick S. Mariano[‡], Melisa McCalman[¶], Jan van Kan[¶], Peter J. Schaap[§2], and Debra Dunaway-Mariano[‡3]

From the [‡]Department of Chemistry, University of New Mexico, Albuquerque, New Mexico 87131, the [§]Laboratory of Microbiology Section Fungal Genomics, Wageningen University, Dreijenlaan 2, 6703 HA Wageningen, The Netherlands, and the [¶]Laboratory of Phytopathology, Wageningen University, Binnenhaven 5, 6709 PD Wageningen, The Netherlands

Oxalate secretion by fungi is known to be associated with fungal pathogenesis. In addition, oxalate toxicity is a concern for the commercial application of fungi in the food and drug industries. Although oxalate is generated through several different biochemical pathways, oxaloacetate acetylhydrolase (OAH)-catalyzed hydrolytic cleavage of oxaloacetate appears to be an especially important route. Below, we report the cloning of the *Botrytis cinerea oahA* gene and the demonstration that the disruption of this gene results in the loss of oxalate formation. In addition, through complementation we have shown that the intact *B. cinerea oahA* gene restores oxalate production in an *Aspergillus niger* mutant strain, lacking a functional *oahA* gene. These observations clearly indicate that oxalate production in *A. niger* and *B. cinerea* is solely dependent on the hydrolytic cleavage of oxaloacetate catalyzed by OAH. In addition, the *B. cinera oahA* gene was overexpressed in *Escherichia coli* and the purified OAH was used to define catalytic efficiency, substrate specificity, and metal ion activation. These results are reported along with the discovery of the mechanism-based, tight binding OAH inhibitor 3,3-difluorooxaloacetate (K_i = 68 nM). Finally, we propose that cellular uptake of this inhibitor could reduce oxalate production.

Numerous filamentous fungi, including the food biotechnology fungus *Aspergillus niger*, the opportunistic human pathogen *Aspergillus fumigatus*, the phytopathogenic fungi *Botrytis cinerea* and *Sclerotinia sclerotiorum*, as well as many brown-rot and white-rot basidiomycetes, are able to efficiently produce large quantities of oxalate (1, 2). It is known that oxalate secretion is associated with fungal pathogenesis (1, 3–6). In the wood-rotting fungus *Fomitopsis palustris* oxalate is formed as the product of glucose metabolism (7). We recently initiated investigations of the oxalate biosynthetic pathway to develop a genomic-based method for distinguishing between oxalate producing and non-producing fungi. An additional goal of this effort was to identify enzyme inhibitors that could be used to arrest oxalate formation in targeted fungi.

To attenuate oxalate production in fungi, it is necessary to first identify the major pathway responsible for oxalate formation. There are three potential routes for production of oxalate in fungi: oxidation of glyoxylate (8, 9), oxidation of glycolaldehyde (10), and hydrolysis of oxaloacetate (11). The results of studies of $[^{14}C]CO_2$ incorporation into the metabolite pools of *A. niger* indicate that oxalate is derived from oxaloacetate (12). This finding parallels the results of earlier work on the purification of an enzyme "oxalacetalase" (now known as oxaloacetate acetylhydrolase or OAH)[4] that catalyzes the hydrolytic cleavage of oxaloacetate to form acetate and oxalate (11). In a subsequent study, a mutant *A. niger* strain, NW228 (13), was found to be deficient in both oxalate production and in the synthesis of active OAH (14). These observations suggest that oxalate is produced only by the OAH catalyzed process. In the present investigation, we verified the connection between the absence of oxalate formation and the absence of OAH activity in the NW228 mutant by demonstrating that the OAH encoding *oahA* gene is interrupted by a stop codon. In an independent effort, Pedersen *et al.* (15) mutated the *A. niger oahA* gene by recombination with an *oahA* sequence-based plasmid, to create a metabolically robust *A. niger* strain deficient in oxalate production.

OAH isolated from *A. niger* is reported to be a mixture of N-terminal truncates (16). To obtain homogeneous OAH, we first cloned the *A. niger oahA* gene for overexpression in *Escherichia coli*. However, we failed to isolate active transformants. Subsequent efforts focused on cloning the *oahA* gene from the alternate fungal source *B. cinerea* (previously known as *Botryotinia fuckeliana*). The cloned *B. cinera oahA* gene was shown to both restore oxalate production in the *A. niger* NW228 mutant strain (13, 14) that lacks a functional *oahA* gene and produce OAH in transformed *E. coli* cells. To provide insight into the mechanism of catalysis and to set the stage for the design of mechanism-based inhibitors, the OAH substrate and metal cofactor specificities were determined. Below we report the results from these studies, which have culminated in the discov-

* This work was supported by National Institutes of Health Grant GM 28688 (to D. D. M.), National Science Foundation Grant CHE055013 (to P. S. M.), and by the Food Technology, Nutrition and Health graduate school (to P. J. S. and H.-J. J.). The costs of publication of this article were defrayed in part by the payment of page charges. This article must therefore be hereby marked "*advertisement*" in accordance with 18 U.S.C. Section 1734 solely to indicate this fact.

[1] Both authors contributed equally to this work.
[2] To whom correspondence may be addressed. Tel.: 31317-485142; Fax: 31317-484011; E-mail: peter.schaap@wur.nl.
[3] To whom correspondence may be addressed. Tel.: 505-277-3383; Fax: 505-277-6202; E-mail: dd39@unm.edu.

[4] The abbreviations used are: OAH, oxaloacetate acetylhydrolase; PEP, phosphoenolpyruvate; DTT, dithiothreitol; HPLC, high performance liquid chromatography.

ery that 3,3-difluorooxaloacetate is a novel tight-binding OAH inhibitor.

EXPERIMENTAL PROCEDURES

Materials

Oxaloacetic acid, (*R*)-malic acid, (*S*)-malic acid, (2*R*)-methylmalic acid, (2*S*)-methylmalic acid, and (2*R*,3*S*)-isocitric acid were purchased from Sigma. (2*R*,3*S*)-2,3-dimethylmalic acid, (2*R*)-ethyl-(3*S*)-methylmalic acid, (2*R*)-propyl-(3*S*)-methylmalic acid, *threo*-(2*R*,3*S* and 2*S*,3*R*)-2-methylisocitrate were prepared according to Ref. 17. (2*R*, 3*S*)-Isopropylmalate (synthesized by M. Jung) and 3-butylmalate (Aldrich Rare Chemicals, number S789046) were provided by S. Clarke (University of California, Los Angeles, CA).

3,3-Difluorooxaloacetate

This compound was prepared by modifying the protocol described by Saxty *et al.* (18). A stirred suspension of zinc powder (6.5 g, 0.1 mol) in anhydrous tetrahydrofuran (50 ml) containing Me_3SiCl (4 ml, 0.04 mol) was stirred at room temperature for 15 min and then at reflux while ethyl bromodifluoroacetate (24.24 g, 0.12 mol) was added. To this solution was added ethyl formylformate (5.2 g, 0.05 mol) at a rate sufficient to maintain gentle reflux. After stirring at reflux for 1 h, the solution was cooled to room temperature and concentrated *in vacuo*. The resulting residue was dissolved in water and then extracted with ethyl acetate. The extracts were washed with water, dried, and concentrated *in vacuo*. The resulting residue was subjected to silica gel column chromatography (methylene chloride and 1:5 ethyl acetate/hexane) to give diethyl 2,2-difluoro-3-hydroxysuccinate (7.9 g, 69%).

To a solution of sulfuric acid (10 ml, 0.18 mol) and pyridinium chlorochromate (0.093 mol) in water (40 ml) was added diethyl 2,2-difluoro-3-hydroxysuccinate (7.0 g, 0.031 mol) dropwise. After stirring at room temperature for 7 h, the mixture was filtered. The filtrate was concentrated *in vacuo* to give a residue, which was subjected to silica gel column chromatography (10:1 to 3:1 ethyl acetate/hexane) to yield homogeneous diethyl 3,3-difluorooxaloacetate (3.75 g, 50%). The spectroscopic data of this substance matched those reported earlier (19); ^{1}H NMR ($CDCl_3$) 1.34 (m, 6H), 4.39 (m, 4H); ^{13}C NMR 167.1, 162.3 (t, J = 31.0 Hz), 110.8 (t, J = 263.5 Hz), 91.9 (t, J = 28.1 Hz), 64.1, 63.7, 13.7.

A mixture of diethyl 3,3-difluorooxalacetate (1.70 g, 7.0 mmol) and 13 ml of 3 M HCl was stirred at reflux for 1.3 h, cooled to room temperature, and concentrated *in vacuo*. Addition of 2 ml of trifluoroacetic acid to the residue resulted in the formation of a solid, which was filtered and dried *in vacuo* to yield 3,3-difluorooxaloacetate (1.18 g, 90%). In agreement with a previous report (19), the ^{13}C NMR (D_2O) spectrum is as follows: 169.9, 165.4 (t, J = 29.4 Hz), 112.0 (t, J = 261.1 Hz), and 92.0 (t, J = 27.2 Hz).

A. niger OAH Gene Cloning and Sequencing

The *oahA* genes from the *A. niger* wild type strain N400 (CBS120.49), and derived mutant strains NW228 (*prtF28*) and NW229 (*prtF29*) (13), were amplified by using standard PCR protocol in conjunction with the forward primer CTGGCCCTTCCTTTCTATC and the reverse primer CCATCCAATGCAGTTCAAC. The PCR products were cloned using the vector pGEM®-T Easy (Promega) and sequenced. The nucleotide sequence of the N400 strain has been deposited in the public data bases under accession number AJ567910.

Cloning of the B. cinerea oahA Gene

The GenomeWalker kit (Clontech) was used to obtain the PCR product of the genomic region containing the OAH encoding gene from *B. cinerea* strain B05.10. The sequences of gene-specific primer 1 (ATCAACACAATATCGGAGTTCATGG) and primer 2 (GCACGAATTCTCATGT-AGTACTCCTCT) were derived from *B. cinerea* EST AL117176. The complete *oah* gene along with 308 bp of the upstream region was amplified, cloned in the vector pGEM-T Easy (Promega), and sequenced. Standard reverse transcriptase-PCR techniques were used to verify the two introns. The nucleotide sequence has been deposited in the public data bases under accession number AY590264.

Complementation of the A. niger prtF Mutation

Three different constructs were made for complementation of the prtF mutation with the *B. cinerea oah* gene. These are the full-length *B. cinerea oah* gene including the 308-bp upstream region and two fusion constructs in which the *A. niger pkiA* (20) promoter was fused to the two possible start codons. All three constructs where co-transformed into strain NW188 (pyrA6, *prtF28*) as previously described (21). Transformants where screened for oxalate production by growing single colonies on complete media (22) plates with 10 ng/ml methyl orange as the pH indicator. Only the transformants in which the *pkiA* promoter was fused to the most upstream start codon showed oxalate production as verified by HPLC analysis. The copy number of OAH *B. cinerea* of the transformants was determined by Southern analysis using the *pkiA* promoter as a radiolabeled probe. The copy number was estimated by comparing the intensity of the native *A. niger* pki promoter band (1 copy) to the intensity of the band of the introduced pkiA-*BcoahA* construct.

Targeted Mutagenesis of B. cinerea

A gene replacement construct containing fragments originating from either end of the *BcoahA* gene flanking a hygromycin resistance cassette (GenBank™ accession AJ439603) was prepared. The 5′-flanking fragment (466 bp) was amplified using the primers CCCAATCCTCCAAGAGAAGTC and GATTACTAACAGATATCAAGGCTTCAAGCGGGAAGCAGTGGTAC. The 3′-flanking fragment (611 bp) was amplified using primers GGGTACCGAGCTGCAATTCGTTGTGGACATCTCCAAGGC and CCAACCAGGTACTGAGATCAG. The flanking fragments were joined to the hygromycin cassette by overlap extension. The PCR mixture contained the three template fragments and primers GACTGCTACTGAGTATTCGGT and CTACTCAAACACCATCCGCGA. The resulting PCR fragment was excised from the gel and directly transformed to *B. cinerea* protoplasts using the published procedure (23).

Purification of Recombinant B. cinerea OAH from the OAH-pET3c E. coli Clone

The OAH encoding gene was amplified by using a PCR-based strategy (24) with the OAH-pGem-T Easy vector clone serving as the template. *Pfu* DNA polymerase (Stratagene) and oligonucleotide primers containing NdeI and BamHI restriction sites were used for the subcloning the OAH gene into the pET-3c vector (Novagen). The recombinant plasmid, OAH-pET3c, was used to transform competent *E. coli* BL21(DE3) cells (Novagen). The transformed cells were grown at 20 °C with mild agitation (180 rpm) in Luria broth containing 50 μg/ml carbenicillin. After 19 h of cell growth ($A_{600\ nm} \sim 0.7$), induction was initiated with 0.4 mM isopropyl β-D-thiogalactopyranoside (RPI Corp.). The culture was incubated for 12.5 h at 20 °C under conditions of vigorous mixing (200 rpm). The cells were harvested by centrifugation (6,500 rpm (7,808 × *g*)) for 15 min at 4 °C in a yield of 4 g/liter of culture media. The cell pellet (23 g) was suspended in 230 ml of ice-cold lysis buffer (50 mM K^+/Hepes (pH 7.5), 1 mM EDTA, 1 mM benzamide hydrochloride, 0.05 mg/ml trypsin inhibitor, 1 mM 1,10-phenanthroline, 0.1 mM phenylmethylsulfonyl fluoride, and 5 mM DTT). The suspension was passed through a French Press at 1,200 p.s.i., and then centrifuged at 4 °C for 60 min at 20,000 rpm (48,384 × *g*). The supernatant was fractionated by ammonium sulfate-induced protein precipitation. The 30–40% ammonium sulfate protein precipitate was dialyzed at 4 °C against 4 × 2 liters of Buffer A (50 mM triethanolamine (pH 7.5), 5 mM $MgCl_2$, and 5 mM DTT) before loading onto a 4.5 × 45-cm DEAE-cellulose column equilibrated with 2 liters of Buffer A. The column was washed with 1 liter of Buffer A, and then eluted with a 2-liter linear gradient of 0 to 0.3 M KCl in Buffer A. The column fractions were analyzed by measuring the absorbance at 280 nm and by carrying out SDS-PAGE analysis. Ammonium sulfate was added to the combined fractions to generate 20% saturation. The resulting solution was loaded onto a 3 × 30-cm Butyl-Sepharose column equilibrated at 4 °C with 20% ammonium sulfate in 500 ml of Buffer A. The column was washed with 450 ml of 20% ammonium sulfate in Buffer A and then eluted with a 1-liter linear gradient of 20 to 0% ammonium sulfate in Buffer A. The column fractions were analyzed by measuring the absorbance at 280 nm and by carrying out SDS-PAGE analysis. The OAH eluted at 4% ammonium sulfate. The OAH-containing fractions were combined, concentrated at 4 °C with an Amicon concentrator (Amicon), and then dialyzed against Buffer A. The resulting sample was concentrated using a MACROSEP 10K OMEGA for storage at −80 °C. The protein sample was shown to be homogeneous by SDS-PAGE analysis with a yield of 4 mg of protein/g wet cell.

Recombinant B. cinerea OAH N-terminal Sequence Determination

OAH was chromatographed on a SDS-PAGE gel, transferred to a polyvinylidene difluoride membrane (Novex Co.) and subjected to automated protein N-terminal amino acid sequencing by Dr. Brian M. Martin of the National Institutes of Mental Health (Molecular Structure Unit, Department of Neurotoxicolgy, Bethesda, MD) to obtain the sequence PAYSDKVMLT.

Recombinant B. cinerea Molecular Mass Determination

The theoretical subunit molecular mass of recombinant OAH was calculated by using the amino acid composition, derived from the gene sequence, and the EXPASY Molecular Biology Server program Compute pI/MW (25). The subunit size of recombinant OAH was determined by SDS-PAGE analysis with molecular weight standards from Invitrogen. The subunit mass was determined by MS-ES mass spectrometry (University of New Mexico Mass Spectrometry Lab). The molecular weight of native recombinant OAH was first determined using gravity flow gel filtration techniques. The chromatography of OAH was carried out with a 1.5 × 180-cm Sephacryl S-200 column (GE Healthcare) equilibrated with Buffer B (25 mM K^+/Hepes, 0.15 M KCl, 0.5 mM DTT, pH 7.5) at 4 °C. The Pharmacia Gel Filtration Calibration Kit (catalase, 232,000; aldolase, 158,000; albumin, 67,000; ovalbumin, 43,000; chymotrypsinogen A, 25,000; ribonuclease A, 13,000) was used to calibrate the column according to the manufacturer's instructions. The chromatography was carried out at 4 °C using Buffer B as eluant and a peristaltic pump to maintain a constant flow rate of 1 ml/min. The plot of the elution volume of the molecular weight standards *versus* log molecular weight was found to be linear. The OAH molecular weight was thus derived from the measured elution volume by extrapolation. OAH native mass was also analyzed at the HHMI Biopolymer/Keck Foundation Biotechnology Resource Laboratory at Yale University by size exclusion chromatography coupled with on-line laser scattering, refractive index, and ultraviolet detection.

Oxaloacetate Hydrolase Assay

OAH activity was assayed according to a published procedure (11). Reaction solutions (1 ml) contained 0.06–1.0 mM oxaloacetate, 0.032 μM OAH, and 5 mM $MgCl_2$ or 0.18–1.2 mM oxaloacetate, 0.011 μM OAH, and 0.3 mM $MnCl_2$ in 0.1 M imidazole (pH 7.6 and 25 °C). The reaction was monitored at 255 nm for the disappearance of the enol tuatomer of oxaloacetate ($\Delta\epsilon = 1.1\ mM^{-1}\ cm^{-1}$). The rate of oxaloacetate consumption via spontaneous decarboxylation was measured prior to initiating the enzymatic reaction to determine the "background rate." The background rate was subtracted from the reaction rate measured in the presence of OAH. The influence of the buffer properties on the OAH kinetic behavior was tested by replacing the 0.1 M imidazole of the reaction solutions with 50 mM K^+/Hepes (pH 7.5) or 50 mM Tris-HCl (pH 7.5).

Assay for Malate Substrates

Continuous Assay—The OAH (13 μM) lyase activity toward 1 mM (*R*)-malate, (*S*)-malate, (2*S*)-methylmalate, (2*R*,3*S*)-isocitrate, *threo*-(2*R*,3*S* and 2*S*,3*R*)-2-methylisocitrate, (2*R*,3*S*)-isopropylmalate, or 3-butylmalate was measured using 1-ml reaction solutions containing 5 mM $MgCl_2$, 20 units/ml lactate dehydrogenase, and 0.2 mM NADH in 50 mM K^+/Hepes (pH 7.5 and 25 °C). The absorbance of the solution was monitored at 340 nm ($\Delta\epsilon = 6.2\ mM^{-1}\ cm^{-1}$). The kinetic constants for OAH lysis of (2*R*)-methylmalate, (2*R*,3*S*)-dimethylmalate, and (2*R*)-ethyl-(3*S*)-methylmalate were determined with assay solutions in which the reactant concentration is varied from 0.5 K_m to 10

K_m. In the case of (2*R*)-ethyl-(3*S*)-methylmalate, reaction solutions contained 600 units of lactate dehydrogenase.

Fixed Time Assay—Reaction solutions initially containing 6 μM OAH, 0.50–3.75 mM (2*R*)-propyl-(3*S*)-methylmalate, 5 mM $MgCl_2$, and 50 mM K^+/Hepes (pH 7.5, 25 °C) were analyzed at ~20% conversion. A 200-μl aliquot was mixed with 200 μl of 1 N HCl and 100 μl of 0.4 M phenylhydrazine hydrochloride. The solution was stirred for 12 min before the absorbance was measured at 326 nm (2-oxovaleric acid hydrazone molar extinction constant is 6.8 mM^{-1} cm^{-1}). The control reaction lacked OAH.

Steady-state Kinetic Constant Determination for Recombinant B. cinerea OAH Substrates

The steady-state kinetic parameters (K_m and k_{cat}) were determined from the initial velocity data measured as a function of substrate concentration. The initial velocity data were fitted to Equation 1 with KinetAsystI,

$$V_0 = V_{max}[S]/(K_m + [S]) \quad \text{(Eq. 1)}$$

where [S] is the substrate concentration, V_0 is the initial velocity, V_{max} is the maximum velocity, and K_m is the Michaelis-Menten constant for the substrate. The k_{cat} value was calculated from V_{max} and the enzyme concentration using the equation $k_{cat} = V_{max}/[E]$, where [*E*] is the protein subunit molar concentration in the reaction calculated from the ratio of measured protein concentration and the protein molecular mass (34,486 Da).

Determination of Inhibition Constants for Recombinant B. cinerea OAH Inhibitors

For determination of the competitive inhibition constant K_i, the 1-ml reaction solutions initially contained 0.1 M imidazole (pH 7.6), 5 mM $MgCl_2$, 9 nM oxaloacetate hydrolase, varying concentrations of oxaloacetate (0.04–1.0 mM) and changing, fixed concentrations of difluorooxaloacetate (0, 0.2, and 0.4 μM), oxalate (0, 25, 50, and 100 μM), (*R*)-malate (0, 10, and 20 mM), or (*S*)-malate (0, 20, and 40 mM). Initial velocity data were fitted to Equation 2.

$$V_0 = V_{max}[S]/(K_m(1 + (I/K_i)) + [S]) \quad \text{(Eq. 2)}$$

Metal Ion Activation of Recombinant B. cinerea OAH

The metal ion-free protein was prepared by dialysis against 7 changes of 500 ml of 30 mM EDTA, 50 mM triethanolamine, 5 mM DTT (pH 7.5, 4 °C) followed by dialysis against 6 changes of 500 ml of 50 mM triethanolamine, 5 mM DTT (pH 7.5, 4 °C). The initial velocity of oxaloacetate consumption in reaction solutions containing OAH, 1 mM oxaloacetate, and varying concentrations of $MgCl_2$, $MnCl_2$, $CoCl_2$, $CaCl_2$, $ZnCl_2$, $FeSO_4$, $CuBr_2$, $NiCl_2$ in 0.1 M imidazole (pH 7.6), 50 mM K^+/HEPES (pH 7.5), or 50 mM Tris-HCl (pH 7.5) at 25 °C. The initial velocity data were analyzed using Equation 1 and the computer program KinetAsystI.

RESULTS

Cloning and Sequencing of the oahA Gene from Oxalate Non-producing Mutant Strains—The *oahA* genes from the *A. niger* mutant strains, *prtF28* (NW228) and *prtF29* (NW229), were sequenced and their sequences were compared with that of the *oahA* gene contained in the wild-type parental strain. Previous studies had shown the mutant strains lack both oxalate production and OAH activity (14, 26). However, it remained to be demonstrated that the *oahA* gene is disrupted. The sequence analysis verified that the *oahA* genes from the mutant strains had acquired a stop codon in the open reading frame (at amino acid positions Arg-94 (NW228) or Gln-159 (NW229)). Furthermore, by using a pH indicator plate assay (Fig. 1) and HPLC analyses (data not shown) we demonstrated that the mutant strains, transformed with the wild type *oahA* gene, regain their oxalate production capability.

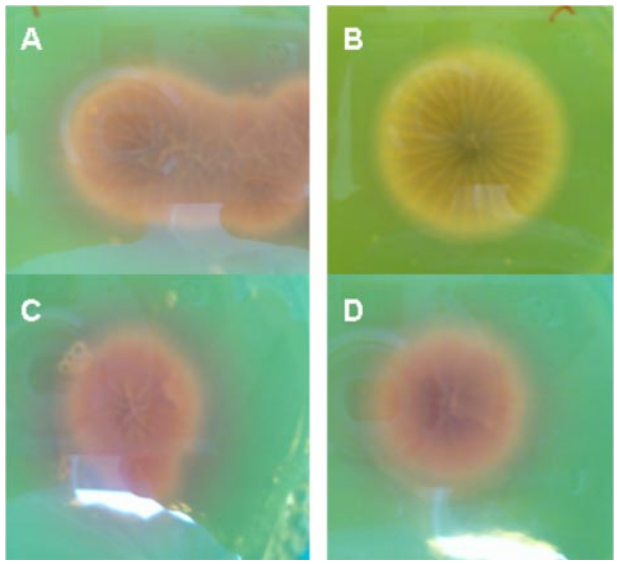

FIGURE 1. **Screen for oxalate production in *A. niger* using a methyl orange pH indicator plate assay.** The *pink* color indicates acidification caused by hydrolytic cleavage of oxaloacetate, which produces oxalate, acetate, and a hydrogen ion. *A*, wild type *A. niger*. *B*, oxalate non-producing mutant NW228. *C*, NW228 transformed with the wild type *A. niger oahA* gene. *D*, NW228 transformed with the *B. cinerea oahA* gene.

Cloning and Disruption of the B. cinerea oahA Gene—The results from the complementation experiment described above strongly suggest that oxalate production in *A. niger* is caused solely by OAH-catalyzed cleavage of oxaloacetate. We scrutinized the genomes of other fungal oxalate producers to see if they too encoded OAH. BLAST searches using the *A. niger oahA* gene (*AnoahA*) as the query suggested that EST AL117176 from the oxalate producer *B. cinerea* represents a partial copy of the *B. cinerea* OAH encoding gene. The complete *BcoahA* gene, isolated from the *B. cinerea* genome by using PCR and genome walking techniques, was then used for complementation of the *prtF28* mutation. The sequence of the putative BcOAH was shown to be 70% identical to that of the *A. niger* OAH. Because there are two possible start codons separated by 7 amino acids, three different constructs were made for complementation purposes. These are the full-length *B. cinerea oahA* gene (including the 308-bp upstream region calculated from the most upstream candidate start codon) and two fusion constructs, in which the constitutive *A. niger pkiA* promoter (20) is fused to one of the two possible start codons. Complementation of the *A. niger* NW228 non-oxalate producing strain was achieved with the *BcoahA* coding region that included the

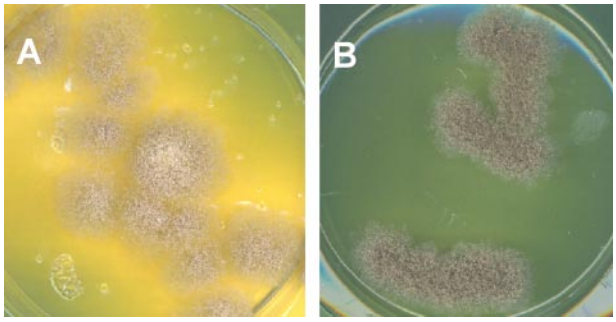

FIGURE 2. **Screen for oxalate production *B. cinerea* using a bromthymol blue pH indicator plate assay.** The *yellow* color indicates acidification caused by the hydrolytic cleavage of oxaloacetate to oxalate, acetate, and a hydrogen ion. *A*, wild type *B. cinerea*. *B*, *oahA* deletion strain.

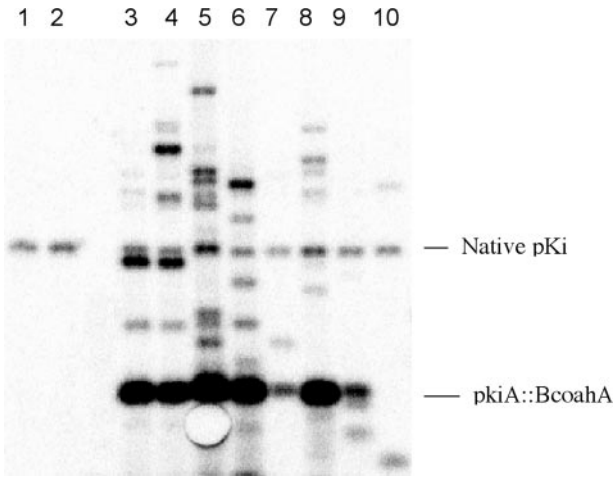

FIGURE 3. **Molecular characterization of *A. niger* NW228 transformants complemented with pkiA::BcoahA construct.** *Lanes 1* and *2*, NW228 control. *Lanes 3–9*, 8 independent NW228 pkiA::BcoahA transformants. *Lane 10*, wild type control. The bands corresponding with the native *pkiA* gene and the construct are indicated.

most upstream start codon fused to the strong *A. niger pkiA* promoter (20). Seven independent *pkiA::BcoahA* transformants were identified by using an indicator plate assay (Fig. 2). The integration of the construct within the transformants was verified by using Southern analysis (Fig. 3). HPLC analysis was used to demonstrate that each transformant had regained the ability to produce oxalate (data not shown).

To confirm the role played by the *Bcoah*A gene in oxalate biosynthesis in *B. cinerea,* the gene was deleted from the *B. cinerea* genome by employing targeted gene replacement. Transformants, in which homologous recombination had occurred, were identified by PCR screening and Southern blot analysis. Five independent transformants were identified as having perfect gene replacement in the absence of additional ectopic integration (data not shown). The pH indicator plate assay (Fig. 2) was used to demonstrate that the *Bcoah*A-deficient mutants do not produce a detectable level of oxalate.

Purification of Recombinant B. cinerea OAH and Size Determination—The DNA sequence of the subcloned gene was found to agree with the published sequence (GenBank accession number AY590264) except that the nucleotide at position 1637 is G not A. Thus, the encoded amino acid is Ala not Thr. The recombinant OAH was purified to homogeneity in an overall yield of 4 mg/g wet cells by using the 4-step protocol

TABLE 1
Experimental protocol for purification of *B. cinerea* OAH from *E. coli* BL21(DE3) cells transformed with the OAH-pET3c clone

Purification step	Total protein	Total activity[a]	Specific activity	Yield	Purification
	g	*units*	*units/mg*	*%*	*-fold*
Cell extract	20	12,300	0.62	100	
Ammonium sulfate	2	11,300	4.6	92	7
DEAE-cellulose	0.35	5,300	15	43	25
Butyl-Sepharose	0.17	3,430	20	28	33

[a] One unit of enzyme activity is defined as the amount of enzyme required for the consumption of 1 μmol of oxaloacetate/min in 0.1 M imidazole, 5 mM $MgCl_2$, and 1 mM oxaloacetate at 25 °C and pH 7.6.

summarized in Table 1. The N-terminal sequence of OAH revealed that the N-terminal methionine is lost during post-translational modification. This was confirmed by a molecular mass determination using mass spectroscopy. The theoretical mass of OAH-Met is 34,355 Da compared with the experimental value of 34,355 ± 1 Da. The SDS-PAGE analysis gave an estimated subunit mass of 35 kDa, whereas the native mass measured by using molecular size gel filtration chromatography is ~100 kDa. This result is indicative of a homotrimeric quaternary structure. The α,β-barrels of the enzymes of the PEP mutase/isocitrate lyase superfamily incorporate the C-terminal α-helix from an adjacent subunit, a family structural trait known as "helix swapping." The functional unit is therefore a dimer, and the quaternary structure that has been most frequently encountered is the homotetramer (Ref. 17 and references therein). Because a trimeric structure is not consistent with this pattern, we examined the possibility that the association state of OAH is unstable. Native molecular mass determination, by using size exclusion chromatography, coupled with on-line laser scattering, refractive index, and ultraviolet detection provided additional information regarding the OAH quaternary structure. A sample of OAH eluted in a single peak from size exclusion fractionation was polydispersed with a molecular mass range of 50 kDa at 0.05 mg/ml to 114 kDa at 0.3 mg/ml and averaged molecular mass of 97 kDa. At 1.1 mg/ml the sample reached an averaged molecular mass of 118 Da and a hydrodynamic radius of 4.1 nm. The hydrodynamic radius remained at 4.1 nm at 3 mg/ml indicating that the protein does not exist in oligomeric forms higher than a tetramer. The results are consistent with the existence of a monomer-dimer-tetramer equilibrium.

Metal Ion Specificity of B. cinerea OAH—Enzymes of the isocitrate lyase/PEP mutase superfamily require a divalent metal ion for catalysis. The steady-state kinetic constants for metal ion activation of OAH were determined at a saturating concentration of oxaloacetate (1 mM) and varying metal ion concentration using 0.1 M imidazole (pH 7.6), 50 mM K^+/Hepes (pH 7.5), or 50 mM Tris-HCl (pH 7.5) as buffer. The k_{cat} and K_a values, measured for the Mg^{2+}, Mn^{2+}, and Ca^{2+} activation are listed in Table 2. Mn^{+2} and Mg^{2+} are significantly better activators for OAH than is Ca^{2+}. The k_{cat} values determined using the 0.1 M imidazole buffer do not differ significantly from those measured using the K^+/Hepes buffer. The K_a values measured using the K^+/Hepes buffer (which does not bind divalent metal ions) are slightly smaller than those measured using the imidazole buffer (which does bind metal ions). OAH is not subject to

TABLE 2

Steady-state kinetic constants for M^{2+}-activated OAH catalyzed hydrolytic cleavage of oxaloacetate at 25 °C

Reaction solutions were buffered with 0.1 M imidazole (pH 7.6), 50 mM K^+/Hepes (pH 7.5) or 50 mM Tris-HCl (pH 7.5). Kinetic constants reported in parentheses represent an independent experimental determination.

Cofactor	Buffer	k_{cat}	K_m OAH[a]	K_a M^{2+}[b]
		s^{-1}	μM	
Mg^{2+}	Imidazole	10.3 ± 0.4	62 ± 5	
	Hepes	9.6 ± 0.3	64 ± 6	
	Tris	9.5 ± 0.4	84 ± 5	
Mg^{2+}	Imidazole	11.8 ± 0.3		76 ± 4
	Hepes	12.5 ± 0.3		43 ± 3
Mn^{2+}	Imidazole	50 ± 1	240 ± 10	
Mn^{2+}	Imidazole	37 ± 1		35 ± 3
	Hepes	32 ± 1		24 ± 3
Ca^{2+}	Imidazole	0.35 ± 0.01		730 ± 90

[a] Reaction solutions contained 0.5–10 × K_m oxaloacetate and 5 mM Mg^+ or 0.3 mM Mn^{2+}.

[b] Reaction solutions contained 1 mM oxaloacetate and 0.5–10 × K_a M^{2+}.

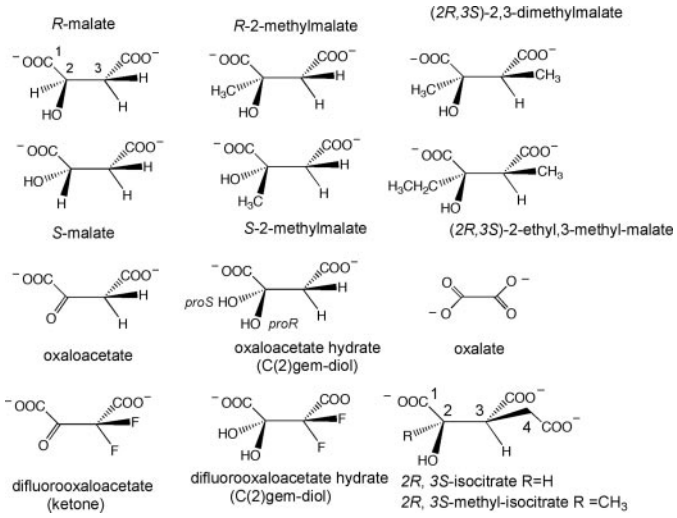

SCHEME 1

metal ion inhibition by Mg^{2+} (no inhibition observed at 5 mM $MgCl_2$). Likewise, inhibition was not observed at 0.3 mM $MnCl_2$. The metal ions Zn^{2+} (100 μM), Co^{2+} (300 μM), Fe^{2+} (100 μM), Cu^{2+} (500 μM), and Ni^{2+} (1 mM) failed to activate OAH.

Substrate Specificity and Kinetic Properties of B. cinerea OAH—The steady-state kinetic constants for OAH-catalyzed hydrolysis of oxaloactate were measured as a function of oxaloacetate concentration at fixed metal ion cofactor concentrations (5 mM $MgCl_2$ or 0.3 mM $MnCl_2$). Reactions were carried out at 25 °C using 0.1 M imidazole (pH 7.6), 50 mM K^+/Hepes (pH 7.5), or 50 mM Tris-HCl (pH 7.5) as buffer. The results are summarized in Table 2. Mn^{2+}-activated OAH displays a higher turnover rate than does the Mg^{2+}-activated OAH. On the other hand, the K_m of oxaloacetate measured by using Mn^{2+} as activator is larger than that measured with Mg^{2+} serving as the activator. Consequently, there is no significant difference in the specificity constant k_{cat}/K_m between Mg^{2+} and the Mn^{2+}-activated OAH.

The ability of OAH to catalyze C–C bond cleavage in α-hydroxycarboxylate metabolites (Scheme 1) was probed to determine whether OAH retains the C–C lyase activity characteristics of the C–C bond lyase branch of the isocitrate lyase/PEP mutase family (*viz.* petal death protein, isocitrate lyase, and 2-methylisocitrate lyase) (Ref. 17 and references therein). The results are listed in Table 3. The first set of substrates tested are the *R*- and *S*-enantiomers of malate. To enhance the sensitivity for detection of product formation, reaction mixtures containing high concentrations of OAH (13 μM) were used. In addition, to ensure saturation of catalytic sites high concentrations (1 mM) of the reactants were employed. Under these conditions, no C–C lyase activity is observed, suggesting that the k_{cat} for cleavage of malate is less than the detection limit that is 1×10^{-5} s^{-1}.

Next, substrate activities of C(2) alkyl malates were probed. Whereas the (2*S*)-methylmalate is not a substrate for OAH, the (2*R*)-methylmalate is converted to pyruvate and acetate with a $k_{cat} = 0.01$ s^{-1} and a $K_m = 1.45$ mM by this enzyme. The addition of a methyl group at the C(3) position of the (2*R*)-methylmalate leads to a further improvement in substrate activity. The K_m value of (2*R*,3*S*)-dimethylmalate is 10-fold smaller than that for (2*R*)-methylmalate. However, the k_{cat} values measured for these two substrates are equivalent. The substrate (2*R*)-ethyl-(3*S*)-methylmalate displayed a 10-fold larger k_{cat} and a comparably larger K_m. The k_{cat}/K_m value measured for (2*R*)-propyl-(3*S*)-methylmalate is significantly smaller (49 M^{-1} s^{-1}), a finding that suggests that the active site has limited space for the C(2) alkyl group.

The native substrates of isocitrate lyase ((2*R*,3*S*)-isocitrate) and 2-methylisocitrate lyase ((2*R*,3*S* and 2*S*,3*R*)-2-methyisocitrate) are not substrates for OAH. This observation indicates that the OAH active site cannot accommodate a C(3) CH_2COO- substituent.

In summary, (2*R*,3*S*)-2,3dimethylmalate and (2*R*)-ethyl-(3*S*)-methylmalate are the most active of the malate substrates tested, each having a k_{cat}/K_m of about 2×10^2 M^{-1} s^{-1}. The petal death protein is known (17) to possess the same substrate specificity: oxaloacetate ($k_{cat}/K_m = 2 \times 10^4$ M^{-1} s^{-1}) and (2*R*)-ethyl-(3*S*)-methylmalate ($k_{cat}/K_m = 2 \times 10^4$ M^{-1} s^{-1}) > (2*R*)-propyl-(3*S*)-methylmalate ($k_{cat}/K_m = 3 \times 10^3$ M^{-1} s^{-1}) > (2*R*)-methylmalate ($k_{cat}/K_m = 7 \times 10^2$ M^{-1} s^{-1}) ⋙ (*R*)-malate and isocitrate. However, the catalytic efficiencies for cleavage of these substrates by the petal death protein are considerably higher than that observed for OAH.

Inhibition of B. cinerea OAH—The competitive inhibition constants of oxalate, (*R*)-malate, (*S*)-malate, and 3,3-difluorooxaloacetate were evaluated to gain information about the structural determinants for ligand binding. Oxalate, a product of oxaloacetate cleavage, binds to OAH with high affinity ($K_i = 19 \pm 1$ μM). Oxalate is also an analog of the pyruvate enolate anion intermediate formed in the cleavage of (2*R*,3*S*)-2,3-dimethylmalate. The petal death protein binds oxalate tightly ($K_i = 4.3 \pm 0.3$ μM), as does isocitrate lyase and PEP mutase (17).

3,3-Difluorooxaloacetate, which differs from oxaloacetate by replacement of the C(3) hydrogens with fluorine atoms, is not a substrate for OAH (the k_{cat} detection limit is 1×10^{-5} s^{-1}). However, this substance is an exceptionally tight binding linear competitive inhibitor: $K_i = 68 \pm 4$ nM) (Fig. 4). In contrast, malate is a weak binding competitive inhibitor of OAH. Malate

TABLE 3

Steady-state kinetic constants determined for the C–C bond cleavage reactions catalyzed by *B. cinerea* OAH in 5 mM $MgCl_2$ and 50 mM K^+/Hepes buffer (pH 7.5 and 25 °C)

Chemical structures are shown in Scheme 1.

Reactant	k_{cat}	K_m	k_{cat}/K_m
	s^{-1}	μM	$M^{-1}\,s^{-1}$
Oxaloacetate	9.9 ± 0.3	65 ± 6	1.5×10^{5} [a]
(2*R*)-Methylmalate	$(1.13 \pm 0.02) \times 10^{-2}$	1450 ± 60	7.8[b]
(2*R*,3*S*)-Dimethylmalate	$(2.93 \pm 0.07) \times 10^{-2}$	140 ± 10	2.1×10^{2} [b]
(2*R*)-Ethyl-(3*S*)-methylmalate	$(3.46 \pm 0.09) \times 10^{-1}$	2000 ± 100	1.7×10^{2} [c]
(2*R*-Propyl-(3*S*)-methylmalate	$(3.77 \pm 0.07) \times 10^{-2}$	770 ± 40	49[d]
(2*R*,3*S*)-Isocitrate	$<10^{-5}$ [b]		
(2*R*,3*S* and 2*S*,3*R*)-2-Methyisocitrate	$<10^{-5}$ [b]		
(*R*)-Malate or (*S*)-malate	$<10^{-5}$ [b]		
(2*S*)-Methylmalate	$<10^{-5}$ [b]		
3-Isopropylmalate	$<10^{-5}$ [b]		
3-Butylmalate	$<10^{-5}$ [b]		

[a] The kinetic constants were determined using direct optical method.
[b] The kinetic constants were determined using lactate dehydrogenase/NADH coupling assay (20 units/ml lactate dehydrogenase).
[c] The kinetic constants were determined by lactate dehydrogenase/NADH coupling assay (600 units/ml lactate dehydrogenase).
[d] The kinetic constants were determined using the fixed time phenylhydrazine-based assay.

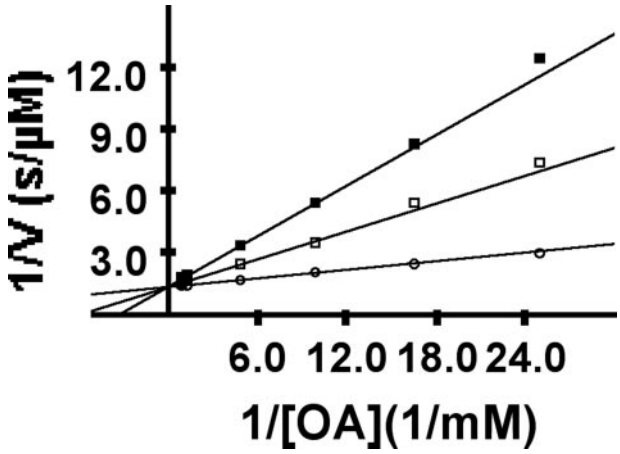

FIGURE 4. **The double-reciprocal plot of the initial velocity of OAH-catalyzed hydrolytic cleavage of oxaloacetate *versus* the concentration of oxaloacetate (0.04–1.0 mM) in 0.1 M imidazole, 5 mM $MgCl_2$ (pH 7.6, 25 °C) at changing, fixed concentrations of difluorooxaloacetate (*circle*, 0 nM; *open square*, 200 nM; *filled square*, 400 nM).** See "Experimental Procedures" for details.

differs from the oxaloacetate in that its C(2) center is tetrahedral and functionalized with a hydroxyl group. (*R*)-Malate (K_i = 2.5 ± 0.2 mM) binds an order of magnitude tighter than does its *S*-enantiomer (K_i = 22 ± 3 mM), but ~5 orders of magnitude less tightly than does 3,3-difluorooxaloacetate.

DISCUSSION

OAH Function and Distribution—The observations described above show that 1) oxalate formation in the fungi *A. niger* and *B. cinerea* derives from OAH-catalyzed hydrolytic cleavage of oxaloacetate; and 2) the respective genomes of *A. niger* and *B. cinerea* contain a single OAH encoding gene. Although, the two OAHs share 70% sequence identity, they display different behavior. The *A. niger* OAH is reported to associate to form high order oligomers and to be specific for Mn^{2+} as the metal ion cofactor. Both enzymes do, however, conserve the active serine residue (Ser-260 of *B. cinerea*) known to contribute significantly to OAH catalytic efficiency.[5]

[5] H. J. Joosten, Y. Han, W. N. Weiling, J. Juan Du, J. Vervoort, D. Dunaway-Mariano, and P. J. Schaap, submitted for publication.

BLAST searches, in which the *A. niger* OAH sequence is used as query, have led to the identification of one or more close homologs (as defined by >50% sequence identity) encoded in the *A. niger* genome, and in the genomes of other *Aspergillus* strains. The homologs of *A. niger* do not posses the active site serine found in authentic OAH. Also, inactivation of the OAH encoding gene results in loss of oxalate formation. Presently, their catalytic functions are unknown.

A. niger and *B. cinerea* are representatives of different subphyla of *ascomycete* fungi, separated by hundreds of millions of years of evolution. Our results strongly suggest that both fungi use OAH catalyzed hydrolytic cleavage of oxaloacetate as the main (if not the sole) route for oxalate production. Among the 22 fungi, whose genomes have been sequenced, the presence of the *oah* gene is strictly correlated with oxalate production.[5] The acquisition of OAH activity in a given fungal species for oxalate production appears to be important for niche adaptation.

We searched for evidence of the occurrence of OAH in organisms from other kingdoms. Earlier reports indicate that oxalate biosynthesis occurs in some plants, especially in plants of the genus *Oxalis* (17, 28–31). Studies carried out with plant tissue extracts indicate that enzyme-catalyzed conversion of oxaloacetate to oxalate does take place (30). However, because of the scarcity of sequenced plant genomes, plant *oah* genes have not yet been identified. One exception is the gene encoding the petal death protein of the flowering plant *Dianthus caryophyllus* (Swiss-Prot entry Q05957). The petal death protein possesses OAH activity in addition to 2-alkylmalate C–C bond lyase activity (27). A BLAST search of the gene data bank, identified homologs of ~60% sequence identity in the plants *Arabidopsis thaliana* and *Oryza sativa.* However, neither of these homologs have been isolated or tested for activity and neither appear to possess an active site Ser, which is well correlated with the presence of OAH activity.[5]

The presence of OAH activity has been observed in extracts of the bacterium *Streptomyces cattleya* (32). Unfortunately, the sequence of the gene associated with this activity has not been reported. To identify other bacterial proteins that might possess OAH activity, we carried out a BLAST search of bacterial genomes using the *D. caryophyllus* petal death protein and the *B. cinerea* OAH as query. The *Bacillus cereus* Swiss-Prot entry

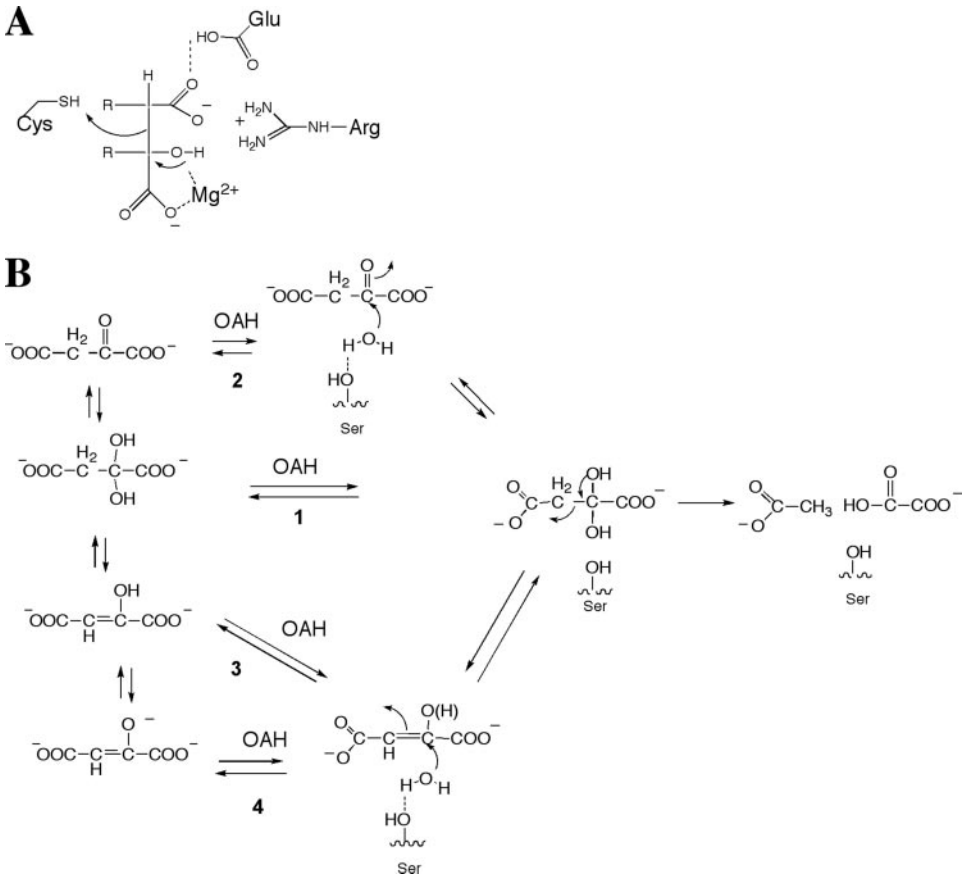

FIGURE 5. *A*, the catalytic mechanism of the α-hydroxycarboxylate lyases of the PEP mutase/isocitrate lyase enzyme superfamily. *B*, the four pathways leading from oxaloacetate to oxalate and acetate.

Q738L6 was found to have the highest homology. This protein is similar in size (*viz.* 302 amino acids) to the petal death protein and the *B. cinerea* OAH. Furthermore, it shares 39% sequence identity with the petal death protein and 36% identity with the *B. cinerea* OAH. However, it does not appear that the *B. cereus* protein contains the conserved active site serine associated with OAH activity.[5] Rather, this protein has a proline residue at this position as do the other bacterial homologs of >35% sequence identity reported to date. The recombinant *B. cereus* Q738L6 was prepared by gene cloning and expression in *E. coli* and the purified enzyme was subjected to substrate screening (33). The *B. cereus* Q738L6 was found to specifically catalyze the cleavage of 2-methylisocitrate to form succinate and pyruvate (k_{cat}/K_m = 2.5 × 10^6 M^{-1} s^{-1}) (33). Thus, the bacterial homolog is not OAH but instead 2-methylisocitrate lyase of the proprionate pathway.

Based on the results of this survey we conclude that OAH is widely used among fungi for the purpose of oxalate formation associated with niche adaptation. Moreover, OAH may also function in oxalate producing plants and perhaps in some specialized bacteria.

OAH Catalysis, Inhibition, and Evolution—OAH catalyzes the hydrolytic cleavage of oxaloacetate (a retro-Claisen reaction) with high efficiency (k_{cat}/K_m = 1.5 × 10^5 M^{-1} s^{-1}) (Table 2). In addition, it promotes retro-Aldol reactions of (2*R*,3*S*)-dimethylmalate and (2*R*)-ethyl-(3*S*)-methylmalate with a 1000-fold lower efficiency (k_{cat}/K_m = 2 × 10^2 M^{-1} s^{-1}) (Table 3). The plant petal death protein displays these same types of catalytic activities but it promotes both processes with equal catalytic efficiency: k_{cat}/K_m = 2 × 10^4 M^{-1} s^{-1} for hydrolytic cleavage of oxaloacetate and for lysis of (2*R*)-ethyl-(3*S*)-methylmalate (17).

OAH and the petal death protein are members of the PEP mutase/isocitrate lyase enzyme superfamily (17, 34–40). Together with isocitrate lyase and 2-methylisocitrate lyase, they form a subgroup of enzymes of similar chemical function. Within this subgroup, the superfamily catalytic scaffold is tailored to bind and activate α-oxocarboxylate metabolites for C(α)–C(β) bond cleavage (17, 35–39). The ability of OAH and the petal death protein to act on C(α)OH and C(α)=O substrates is quite remarkable. This dual catalytic activity might also be possible for isocitrate lyase, but to our knowledge this has not been tested.

The catalytic mechanism that has been proposed for the isocitrate and 2-methylisocitrate lyases is depicted in Fig. 5 (39). The key elements of catalysis are 1) electron withdrawal from the C(α) oxygen via electrostatic interaction with the Mg^{2+} cofactor and the conserved Arg residue; 2) electron withdrawal from the acicarboxylate leaving group via hydrogen bond formation with the conserved glutamic acid residue; 3) general acid catalysis by the conserved Cys residue; and 4) general base catalysis by a yet to be assigned residue.

These elements are conserved in the petal death protein for which the active site structure is known (27). Although the x-ray structure of OAH is not yet available, it is evident from sequence alignment analysis that these same elements contribute to the OAH catalysis. Thus, the catalytic mechanism proposed for the isocitrate and 2-methylisocitrate lyases could be operative in the petal death protein and OAH-mediated cleavage reactions of the (2*R*)-alkylmalates. It is tempting to assume that the OAH catalytic scaffold is designed to promote reaction by way of a single catalytic mechanism (Fig. 5, *pathway 1*). If so, the only adjustment required for operation of a retro-Aldol type mechanism would be the hydration of oxaloacetate to generate the C(α) *gem*-diol. The C(α) *gem*-diol is expected to bind in the active site in the same manner as do (2*R*)-alkylmalates with the pro-S OH of the *gem*-diol located in place of the C(α) alkyl groups of the malates. Modeling studies indicate that Ser-257 in the petal death protein is properly positioned for interaction with the pro-S OH of the oxaloacetate hydrate.[5] The corresponding residue in OAH is Ser-260.

Although the economy of this hydrate/retro-Aldol type mechanism is noteworthy, proof of its operation is needed. In theory, the OAH-catalyzed oxaloacetate cleavage reaction might proceed by any one of several reasonable chemical pathways (Fig. 5, *pathways 1–4*), each of which is distinguished by the form of the oxaloacetate that serves as substrate. In aqueous solution at neutral pH, the keto form of oxaloacetate (81%) exists in equilibrium with the hydrate form (*i.e.* the *gem*-diol) (7%) and the enol form (12%) (41). Oxaloacetate binds Mg^{2+} (and Mn^{2+}) (42). Consequently the ratio of the structural forms at equilibrium is changed, and because of the reduction in pK_a, the enolate form may also contribute to this equilibrium (42). At the current time, it is not clear whether the "free" enzyme binds the Mg^{2+}(oxaloacetate) complex or the enzyme-Mg^{2+} complex binds the free oxaloacetate. Furthermore, the structural form of the oxaloacetate (ketone, *gem*-diol, enol, or enolate) that is bound in the enzyme active site is not known. Therefore, each of the 4 chemical pathways depicted in Fig. 5*B* must be considered.

Whereas the *gem*-diol is a minor component of solvated oxaloacetate, it is the major component by far of solvated 3,3-difluorooxalacetate. In the latter case, only the *gem*-diol is observed by the ^{13}C NMR. However, the report that aspartate transaminase slowly catalyzes the conversion of difluorooxalacetate to difluoroaspartate (43) suggests that the ketone form is present, if only in a trace amount. The high affinity exhibited by OAH for the competitive inhibitor 3,3-difluorooxalacetate (K_i = 68 nM; Fig. 4) suggests that the enzyme preferentially binds the *gem*-diol form of oxaloacetate. Importantly, the *gem*-diol of oxaloacetate serves as a substrate in pathway 1 (Fig. 5*B*), and as an intermediate in pathways 2 and 3. Only in pathway 4, involving the oxaloacetate enolate, does the *gem*-diol not serve as an intermediate. Interestingly, the electrostatic forces that are needed to stabilize the oxyanion intermediate formed in pathway 4, are not required to bind the *gem*-diol intermediate in pathways 1–3. The results of earlier isotope labeling studies, carried out with the OAH from *A. niger*, provide evidence that catalysis by this enzyme does not take place through the enol (or enolate) (11). Specifically, the acetate derived from OAH-catalyzed conversion of the oxaloacetate generated *in situ* by malate dehydrogenase catalysis of *S*-malate uniformly labeled with ^{14}C in a mixture with *S*-malate doubly labeled with tritium at C(2), was found to have a $^{3}H/^{14}C$ ratio twice that of the starting *S*-malate. Enolization of the oxaloacetate would result in loss of one tritium and the formation of acetate that has the same $^{3}H/^{14}C$ ratio as the starting malate. Thus, it appears that pathways 3 and 4 are not followed in the catalytic process.

Based on the fact that pathway 1 is followed in catalysis of the C(α)–C(β) bond cleavage reactions of (2*R*)-alkylmalates and that pathway 2 requires that the enzyme binds and activates a water molecule for nucleophilic attack at the C(α) = O, we propose that the *gem*-diol retro-Aldol pathway is the most reasonable mechanism for the OAH catalyzed transformation of oxaloacetate to oxalate and acetate. However, detailed studies are required to provide definitive proof for this mechanism.

Acknowledgments—We thank Dr. Brian M. Martin of the National Institutes of Mental Health for determination of the OAH N-terminal sequence, and Dr. Steve Clarke and Darren Dumlao of the Department of Chemistry and Biochemistry, UCLA, for samples of (2R,3S)-3-isopropylmalate and 3-butylmalate.

REFERENCES

1. Dutton, M. V., and Evans, C. S. (1996) *Can. J. Microbiol.* **42,** 881–895
2. Gadd, G. M. (1999) *Adv. Microb. Physiol.* **41,** 47–92
3. Nakagawa, Y., Shimazu, K., Ebihara, M., and Nakagawa, K. (1999) *J. Infect. Chemother.* **5,** 97–100
4. Godoy, G., Steadman, J. R., Dickman, B., and Dam, R. (1990) *Physiol. Mol. Plant. Pathol.* **37,** 179–191
5. Guimaraes, R. L., and Stotz, H. U. (2004) *Plant Physiol.* **136,** 3703–3711
6. Kirkland, B. H., Eisa, A., and Keyhani, N. O. (2005) *J. Med. Entomol.* **42,** 346–351
7. Munir, E., Yoon, J. J., Tokimatsu, T., Hattori, T., and Shimada, M. (2001) *Proc. Natl. Acad. Sci. U. S. A.* **98,** 11126–11130
8. Maxwell, D. P., and Bateman, D. F. (1968) *Phytopathology* **58,** 1635–1642
9. Balmforth, A. J., and Thomson, A. (1984) *Biochem. J.* **218,** 113–118
10. Hammel, K. E., Mozuch, M. D., Jensen, K. A., Jr., and Kersten, P. J. (1994) *Biochemistry* **33,** 13349–13354
11. Lenz, H., Wunderwald, P., and Eggerer, H. (1976) *Eur. J. Biochem.* **65,** 225–236
12. Kubicek, C. P., Schreferl-Kunar, G., Wohrer, W., and Rohr, M. (1988) *Appl. Environ. Microbiol.* **54,** 633–637
13. Van den Hombergh, J. P., Van de Vondervoort, P. J., Van der Heijden, N. C., and Visser, J. (1995) *Curr. Genet.* **28,** 299–308
14. Ruijter, G. J., van de Vondervoort, P. J., and Visser, J. (1999) *Microbiology* **145,** 2569–2576
15. Pedersen, H., Christensen, B., Hjort, C., and Nielsen, J. (2000) *Metab. Eng.* **2,** 34–41
16. Pedersen, H., Hjort, C., and Nielsen, J. (2000) *Mol. Gen. Genet.* **263,** 281–286
17. Lu, Z., Feng, X., Song, L., Han, Y., Kim, A., Herzberg, O., Woodson, W. R., Martin, B. M., Mariano, P. S., and Dunaway-Mariano, D. (2005) *Biochemistry* **44,** 16365–16376
18. Saxty, B. A., Novelli, R., Dolle, R. E., Kruse, L. I., Reid, D. G., Camilleri, P., and Wells, T. N. C. (1992) *Eur. J. Biochem.* **202,** 889–896
19. Alberg, D. G., Lauhon, C. T., Nyfeler, R., Fassler, A., and Bartlett, P. A. (1992) *J. Am. Chem. Soc.* **114,** 3535–3546
20. De Graaff, L., van den Broeck, H., and Visser, J. (1992) *Curr. Genet.* **22,** 21–27
21. Kusters-van Someren, M. A., Harmsen, J. A., Kester, H. C., and Visser, J. (1991) *Curr. Genet.* **20,** 293–299
22. Pontecorvo, G., Roper, J. A., Hemmons, L. M., Macdonald, K. D., and Bufton, A. W. (1953) *Adv. Genet.* **5,** 141–238
23. Kars, I., Wagemakers, C. A. M., McCalman, M., and van Kan, J. A. L. (2005) *Mol. Plant Pathol.* **6,** 641–652
24. Erlick, H. A. (ed) (1992) *PCR Technology Principles and Applications for DNA Amplication*, W. H. Freeman and Co., New York
25. Appel, R. D., Bairoch, A., and Hochstasser, D. F. (1994) *Trends Biochem. Sci.* **19,** 258–260
26. Homberg, U., Hoskins, S. G., and Hildebrand, J. G. (1995) *Cell Tissue Res.* **279,** 249–259
27. Teplyakov, A., Liu, S., Lu, Z., Howard, A., Dunaway-Mariano, D., and Herzberg, O. (2005) *Biochemistry* **44,** 16377–16384
28. Weir, T. L., Bais, H. P., Stull, V. J., Callaway, R. M., Thelen, G. C., Ridenour, W. M., Bhamidi, S., Stermitz, F. R., and Vivanco, J. M. (2006) *Planta* **223,** 785–795
29. Guo, Z., Tan, H., Zhu, Z., Lu, S., and Zhou, B. (1999) *Plant Physiol. Biochem.* **41,** 47–92
30. Chang, C., and Beevers, H. (1968) *Plant Physiol.* **43,** 1821–1828
31. Millerd, A., Morton, R. K., and Wells, R. E. (1963) *Biochem. J.* **88,** 276–281
32. Houck, D. R., and Inamine, E. (1987) *Arch. Biochem. Biophys.* **259,**

58–65
33. Han, Y. (2006) *Structure-Function Analysis of the PEP Mutase/Isocitrate Lyase Enzyme Superfamily*, Ph.D. thesis, University of New Mexico
34. Huang, K., Li, Z., Jia, Y., Dunaway-Mariano, D., and Herzberg, O. (1999) *Structure Fold. Des* **7,** 539–548
35. Chaudhuri, B. N., Sawaya, M. R., Kim, C. Y., Waldo, G. S., Park, M. S., Terwilliger, T. C., and Yeates, T. O. (2003) *Structure* (*Camb.*) **11,** 753–764
36. Britton, K., Langridge, S., Baker, P. J., Weeradechapon, K., Sedelnikova, S. E., De Lucas, J. R., Rice, D. W., and Turner, G. (2000) *Structure Fold. Des* **8,** 349–362
37. Sharma, V., Sharma, S., Hoener zu Bentrup, K., McKinney, J. D., Russell, D. G., Jacobs, W. R., Jr., and Sacchettini, J. C. (2000) *Nat. Struct. Biol.* **7,** 663–668
38. Grimm, C., Evers, A., Brock, M., Maerker, C., Klebe, G., Buckel, W., and Reuter, K. (2003) *J. Mol. Biol.* **328,** 609–621
39. Liu, S., Lu, Z., Han, Y., Melamud, E., Dunaway-Mariano, D., and Herzberg, O. (2005) *Biochemistry* **44,** 2949–2962
40. Chen, C. H., Han, Y., Niu, W., Kulakova, A. N., Howard, A., Quinn, J. P., Dunaway-Mariano, D., and Herzberg, O. (2006) *Biochemistry* **45,** 11491–11504
41. Emly, M., and Leussing, D. L. (1981) *J. Am. Chem. Soc.* **103,** 628–634
42. Mao, H. K., and Leussing, D. L. (1981) *Inorg. Chem.* **20,** 4240–4247
43. Briley, P. A., Eisenthal, R., Harrison, R., and Smith, G. D. (1977) *Biochem. J.* **161,** 383–387